IBRO Neuroscience Reports 12 (2022) 355–365

Contents lists available at ScienceDirect

IBRO Neuroscience Reports

journal homepage: www.sciencedirect.com/journal/IBRO-Neuroscience-Reports

Furosemide prevents membrane KCC2 downregulation during convulsant stimulation in the hippocampus

Lulan Chen [a,1], Jiangning Yu [a,1], Li Wan [a,c,1], Zheng Wu [a], Guoxiang Wang [a], Zihan Hu [b], Liang Ren [a], Jing Zhou [a,c], Binbin Qian [a], Xuan Zhao [b,**], Jinwei Zhang [d], Xu Liu [a,***], Yun Wang [a,*]

[a] Department of Neurology, Institutes of Brain Science, State Key Laboratory of Medical Neurobiology and MOE Frontiers Center for Brain Science, Institute of Biological Science, Zhongshan Hospital, Fudan University, Shanghai 200032, China
[b] Department of Anesthesiology, Shanghai Tenth People's Hospital, Tongji University School of Medicine, Shanghai, China
[c] Rehabilitation Center, Shenzhen Second People's Hospital/ the First Affiliated Hospital of Shenzhen University Health Science Center, Shenzhen 518035, China Institute of
[d] Biomedical and Clinical Sciences, Medical School, College of Medicine and Health, University of Exeter, Hatherly Laboratories, Exeter EX4 4PS, UK

ARTICLE INFO

Keywords:
KCC2
Furosemide
$GABA_AR$
Epilepsy

ABSTRACT

In adults, γ-aminobutyric acid (GABA) type A receptor ($GABA_AR$)-mediated inhibition depends on the maintenance of low intracellular chloride anion concentration through neuron-specific potassium-chloride cotransporter-2 (KCC2). KCC2 has been widely reported to have a plasticity change during the course of epilepsy development, with an early downregulation and late recovery in neuronal cell membranes after epileptic stimulation, which facilitates epileptiform burst activity. Furosemide is a clinical loop diuretic that inhibits KCC2. Here, we first confirmed that furosemide pretreatment could effectively prevented convulsant stimulation-induced neuronal membrane KCC2 downregulation in the hippocampus in both in vivo and in vitro cyclothiazide-induced seizure model. Second, we verified that furosemide pretreatment rescued KCC2 function deficits, as indicated by E_{GABA} depolarizing shift and $GABA_AR$ inhibitory function impairment induced via cyclothiazide treatment. Further, we demonstrated that furosemide also suppressed cyclothiazide-induced epileptiform burst activity in cultured hippocampal neurons and lowered the mortality rate during acute seizure induction. Overall, furosemide prevents membrane KCC2 downregulation during acute seizure induction, restores KCC2-mediated GABA inhibition, and interrupts the progression from acute seizure to epileptogenesis.

Introduction

Epilepsy is one of the most common neurological disorders. To facilitate the development of novel therapies, its basic mechanism must be elucidated (Jefferys, 1990). Despite decades of study, the mechanisms underlying epileptogenesis are still not fully understood; an imbalance between excitation and inhibition is likely the underlying cause (McCormick and Contreras, 2001). γ-aminobutyric acid (GABA) type A receptor ($GABA_AR$)-mediated inhibition depends on the maintenance of intracellular [Cl^-] concentration at low levels, which is regulated by K+ -Cl- cotransporter-2 (KCC2) (Ben-Ari, 2002; Farrant and Nusser, 2005; Jacob et al., 2008; Kahle et al., 2008; Rivera et al., 1999). KCC2 is a neuron-specific Cl^- extruder and one of nine cation-chloride co-transporters encoded by *SLC12* genes. Progressive postnatal KCC2 upregulation is associated with maturation of hyperpolarizing inhibition. It shifts E_{GABA} from depolarization to hyperpolarization, which switches $GABA_AR$ function from mediating excitation toward inhibition (Rivera et al., 1999). During epileptogenesis, various studies suggest that KCC2 go through a dynamic plasticity change with an early downregulation and late recovery in neurons. A strong decrease in KCC2 expression associated with the induction of epileptiform activity has been observed in epilepsy animal models (Lee et al., 2010a; Pathak

* Correspondence to: Institutes of Brain Science, Fudan University, Shanghai 200032, China.
** Correspondence to: Department of Anesthesiology, Shanghai Tenth People's Hospital, China.
*** Correspondence to: Department of Neurology, Zhongshan Hospital, Fudan University, China.
E-mail addresses: zhaoxuan1026@hotmail.com (X. Zhao), liu.xu@zs-hospital.sh.cn (X. Liu), yunwang@fudan.edu.cn (Y. Wang).
[1] Lulan Chen, Li Wan, and Jiangning Yu contributed equally to this work

https://doi.org/10.1016/j.ibneur.2022.04.010
Received 10 January 2022; Received in revised form 15 April 2022; Accepted 25 April 2022
Available online 28 April 2022

et al., 2007; Rivera et al., 2002) and human temporal lobe epilepsies (Cohen et al., 2002; Huberfeld et al., 2008, 2007; Palma et al., 2006). *In vitro*, elevation of pathological-like neuronal activity initiates rapid KCC2 withdrawal from neuronal membranes (Chamma et al., 2013; Lee et al., 2011, 2010a, 2007; Puskarjov et al., 2012; Rivera et al., 2004; Wake et al., 2007). Our previous studies (Chen et al., 2017; Wan et al., 2018) have further elucidated that KCC2 downregulation is not only a consequence of but also a contributor to epileptogenesis. Activity-dependent KCC2 downregulation and E_{GABA} depolarization shifts occurred before burst discharge generation. Therefore, KCC2 maintains the normal inhibitory function of $GABA_AR$ and controls epileptogenesis. Maintaining KCC2 expression or function during epileptic activity could mitigate or even terminate epileptogenesis.

Blocking KCC2 reduces the strength of $GABA_AR$ mediated inhibition. Selective inhibitor of KCC2, VU0463271, has been reported to cause a reversible depolarizing shift in E_{GABA} values, increase spiking of cultured hippocampal neurons, and facilitate unremitting epileptiform activity in brain slices exposed to low-Mg^{2+} conditions(Sivakumaran et al., 2015). Furosemide (FUR) is a loop diuretic and a reversible inhibitor of KCC2 and Na^+-K^+-Cl^- cotransporter-1 (NKCC1) (Loscher et al., 2013). It has also been reported that FUR could cause E_{GABA} positive shifts (Barmashenko et al., 2011; Pathak et al., 2007) and induce seizures in vivo (Inoue et al., 1989; Luszczki et al., 2007). However, certain early studies showed that FUR application actually had anticonvulsant efficacy in vitro (Gutschmidt et al., 1999; Hochman and Schwartzkroin, 2000; Margineanu and Klitgaard, 2006) and in vivo (Ahmad et al., 1976; Haglund and Hochman, 2005; Hesdorffer et al., 2001; Hochman et al., 1995; Reid et al., 2000; Yamada et al., 2013). It is supposed that FUR may suppress nonsynaptic synchronization but enhance synaptic excitability by altering ion concentration, osmolality, or pH of the extracellular space (ECS) (Hochman et al., 1995, 1999). Alternatively, FUR may enhance the function of astrocytes rather than neurons (Barbaro et al., 2004). Hence, the precise effects and mechanisms of FUR in this context remain unclear.

Although FUR reversibly inhibits KCC2 function, its effects on membrane KCC2 (mKCC2) expression are unknown. In our previous research, we found that the convulsant cyclothiazide (CTZ) induced robust epileptiform activity and mKCC2 downregulation in hippocampal neurons in vitro and in vivo (Chen et al., 2017; Kong et al., 2010; Qi et al., 2006; Wang et al., 2009). The epileptiform activity had long durations even after CTZ was washed out (Qi et al., 2006). FUR seemed to prevent KCC2 downregulation by CTZ(Wan et al., 2020). In this study, we aimed to further investigate the effects of FUR on mKCC2 levels with and without CTZ-induced seizures using western blot (WB) and immunostaining. We further explored the effects of FUR pretreatment on KCC2 functional deficits using patch clamp recordings, and characterized whether FUR pretreatment influenced CTZ-induced epileptiform activity and seizure behavior using patch clamp recordings and a behavior assay, respectively. This study may provide a new avenue for interrupting epileptogenesis in the acute phase by blocking mKCC2 downregulation.

Materials and methods

Ethical approval

All animal experiments were approved by the Local Committee of the Use of the Laboratory Animals of Fudan University, Shanghai, China. They were conducted in accordance with the guidelines and regulations of the National Natural Science Foundation of China Animal Research.

Animal surgery and behavior assays

Freely moving adult male but not female Sprague–Dawley (SD) rats (220–300 g body weight) were used to establish a CTZ-induced seizure behavioral animal model as previously described (Kong et al., 2010), and avoid the effect of estrogen change during period on eplilepsy (Liu et al., 2013). The rats were anesthetized with chloral hydrate (350 mg/kg, intraperitoneally [i.p.]) and mounted in a stereotaxic apparatus. Their body temperature was maintained at 37 °C. To prepare for intracerebroventricular (i.c.v.) drug administration, a guide cannula (22 GA) was stereotaxically inserted into the left cerebroventricles (AP −0.3 mm, mL 1.3 mm, DP 4.0 mm) and fixed along with the cannula to the skull with dental cement. After surgery, the animals were allowed to recover for at least 5-day before experiments began. The cannula-implanted animals were randomly divided into the following experimental groups for further experiments: 1) Dimethyl sulfoxide (DMSO) group, 2) FUR group,:3) CTZ group: 4) FUR + CTZ group.

The behavioral manifestations of the seizures were rated according to Racine's classification (Racine et al., 1972), which were as RI: chewing, blinking, facial or beard trembling, twitching, stare, dazes; RII: head nodding, repeated scratching, circling, and wet dog shaking; RIII: unilateral forelimb clonus, tail erecting, and back arching; RIV: rearing with bilateral forelimb clonus; and RV: rearing and falling (loss of postural control).

Starting at needle retention, animal behavior was continuorsly observed for 1.5 h, and then a single dose of the chloral hydrate (350 mg/kg, intraperitoneally, i.p.) was injected to terminate, if any, the seizure behaviors as a standard procedure for seizure model establishment. After fully awaken, the animals were then returned to their home cage for another 22.5 h. At 24 h post-CTZ injection, the animals were anesthetized with chloral hydrate (350 mg/kg, i.p.) and then killed, their brains harvested, and the hippocampi were used in the subsequent WB experiments.

Cell culture

Primary hippocampal neurons were prepared using embryonic day 18 SD rats as previously reported (Liu et al., 2013). Pup hippocampi were dissected for tissue preparation. The tissues were rinsed in cold Hanks' balanced salt solution and digested with 0.05% (w/v) trypsin-ethylenediaminetetraacetic acid in a 37 °C incubator for 15–20 min. Single cells were isolated by trituration with a 1-mL plastic pipette tip. After rinsing with Hanks' balanced salt solution, the cells were collected by centrifugation at 1000 rpm for 8 min and resuspended in neuronal medium. The cells were plated onto poly D-lysine-precoated glass coverslips at a density of 30,000–40,000/cm^2. After culturing for 1 d, half the medium was replaced with neurobasal medium supplemented with 2% (w/v) B-27 (Thermo Fisher Scientific, Waltham, MA, USA) and 25 U/mL penicillin/streptomycin. The cells were grown at 37 °C in a 95% O_2/5% CO_2 incubator and fed twice weekly thereafter. Arabinofuranosylcytosine (Ara-C; 2 mm; Sigma-Aldrich Corp., St. Louis, MO, USA) was added 6–8 d after plating. The neurons were used in the subsequent experiments at 11–14 days in vitro (DIV).

Brain slice preparation

Hippocampal slices were prepared from SD rats. Postnatal rats (male, age 21–28 d) were deeply anesthetized and the brains were harvested. The hippocampi were rapidly excised and immersed in an ice-cold, pre-oxygenized solution composed of 119 mM NaCl, 2.5 mM KCl, 2.5 mM $CaCl_2$, 1.3 mM $MgSO_4$, 1 mM NaH_2PO_4, 26.2 mM $NaHCO_3$, and 11 mM glucose. The pH was 7.3 and the osmolality was ~305 mOsm. Slices 300 μm thick were cut with a vibratome (Leica-1200; Leica Microsystems, Wetzlar, Germany) and collected in the aforementioned solution. The slices were incubated for 30 min at 34 °C and recovered at room temperature (RT) for 1 h.

Electrophysiological recording

Hippocampal slices were transferred to a submerged recording chamber and perfused with ACSF at 2 mL/min. The slices were

visualized with infrared optics under a Nikon FN-TP microscope (Nikon Corp., Tokyo, Japan) fitted with DIC optics.

Whole-cell patch recordings were made using the CA1 pyramidal neurons in the brain slices as previously described (Chen et al., 2017). A small patch pipette was extruded from borosilicate glass and polished to 10–14 MΩ resistance. For E_{GABA} recording, the brain slices were incubated with DMSO (0.1% v/v), CTZ (50 μM), FUR (100 μM), or CTZ + FUR for 2 h. The E_{GABA} for the DMSO, CTZ, and FUR + CTZ groups were recorded in drug-free ACSF. The E_{GABA} for the FUR group was recorded in FUR-containing ACSF. The patch pipette was filled with an internal solution consisting of 125 mM K-gluconate, 10 mM KCl, 10 mM HEPES, 4 mM Mg-ATP, 0.5 mM EGTA, 0.5 mM Na_2GTP, and 10 mM Na_2-phosphocreatine. The pH was adjusted to 7.3 with KOH, and the osmolality was ~300 mOsm. Postsynaptic GABA currents were evoked by puffing GABA solution (250 μM) into a CA1 pyramidal cell at holding potentials increasing from − 80 mV to + 40 mV in 10 mV increments. Linear regression was used to plot a best-fit line for the voltage dependence as a function of the evoked GABA current amplitude. The line intersecting the abscissa was taken as the E_{GABA} value.

For the miniature inhibitory postsynaptic current (mIPSC) recordings, patch pipettes were filled with an internal solution with the following composition: 140 mM CsCl, 2 mM $MgCl_2$, 10 mM HEPES, 2 mM Mg-ATP, 0.5 mM Na-GTP, and 10 mM Na_2-phosphocreatine. The pH was adjusted to 7.3 with KOH and the osmolality was ~300 mOsm. Glutamate receptor-mediated synaptic currents were blocked by adding 10 μM DNQX (6,7-dinitroquinoxaline-2,3(1 H,4 H)-dione) and 25 μM AP5 (DL-2-amino-5-phosphonopentanoic acid) to the ACSF. Action potentials of all cells were blocked by adding 1 μM tetrodotoxin to the ACSF. The membrane-impermeable sodium channel blocker QX-314 (lidocaine *N*-ethyl bromide; 10 μM) was added to the internal solution to further prevent the clamped cell from firing action potentials. Although QX-314, a membrane impermeable, quaternary derivative of lidocaine, is also considered to have the KCC2 inhibition property, if acting intracellularly, similar as the membrane permeable lidocaine analog (LH-HCL) and lidocaine (Nakahata et al., 2010), the concentration for QX-314 used in our current study is at least one-fold lower than its functional concentration (μM vs mM) on internal site of KCC2.

Epileptiform activity in the cultured hippocampal neurons was recorded as previously described (Chen et al., 2017). In brief, DIV 11 hippocampal neurons in growth medium were treated with DMSO (0.1% v/v) control, CTZ (5 μM), or FUR (100 μM) + CTZ (5 μM) for 48 h. Coverslips were transferred to a recording bath solution containing 128 mM NaCl, 30 mM glucose, 25 mM HEPES, 5 mM KCl, 2 mM $CaCl_2$, and 1 mM $MgCl_2$. The pH was adjusted to 7.3 with NaOH, and the osmolality was ~320 mOsm. Patch pipettes were filled with an internal solution with the following composition: 125 mM K-gluconate, 10 mM KCl, 2 mM EGTA, 10 mM Hepes, 10 mM Tris-phosphocreatine, 4 mM Mg-ATP, 5 mM EGTA, and 0.5 mM Na_2GTP. The pH was adjusted to 7.3 with KOH, and the osmolality was ~305 mOsm. Whole-cell recording of spontaneous activity was performed in current clamp mode, and the membrane potential was held at − 70 mV. An epileptiform burst is defined as having at least five consecutive action potentials overlaying a large depolarization shift with over 10 mV in amplitude and at least 300 ms long.

Electrical signals were digitized and sampled at 50 μs intervals using a Digidata 1440 A and Multiclamp 700B amplifier (Molecular Devices LLC, San Jose, CA, USA). Data were filtered at 1 kHz and analyzed with pCLAMP v. 10.2 and mini-analysis software.

Immunochemistry

Brain slices

Experiments were performed on hippocampal slices incubated in DMSO (0.1% v/v), CTZ (50 μM), FUR (100 μM), or CTZ (50 μM) + FUR (100 μM) for 2 h. Slices were fixed with 4% (v/v) paraformaldehyde (PFA; pH 7.4) at 4 °C overnight. After dehydration in 30% (w/v) sucrose, the slices were cut into 30-μm sections that were thoroughly rinsed in Tris-buffered saline (TBS), permeabilized, and blocked for 2 h in 0.2% (v/v) Triton X-100% and 10% (v/v) normal donkey serum (NDS) in TBS at RT. The sections were incubated with primary antibody (anti-KCC2, 1:300; EMD Millipore, Billerica, MA, USA) diluted in 10% (v/v) NDS overnight. After several rinses in TBS, the sections were incubated with secondary antibodies for 2 h (donkey anti-rabbit conjugated to Alexa Fluor 488; Molecular Probes, Eugene, OR, USA) diluted in 10% (v/v) NDS at RT. The sections were then rinsed several times in TBS for ≥ 30 min each time and mounted on slides using the Fluoromount (Sigma-Aldrich Corp.). The sections were then viewed under an Olympus FV1000 confocal microscope with 60 × oil immersion objective, and the images were analyzed with Olympus Fluoview v.1.6a (Olympus Corp., Tokyo, Japan).

Cultured neurons

Neurons (DIV 11) were incubated in DMSO (0.1% v/v) control, CTZ (5 μM), FUR (100 μM), or FUR (100 μM) + CTZ (5 μM) for 48 h. They were then rinsed once with TBS and fixed with 4% (v/v) PFA in 0.1 M phosphate buffer (pH 7.4) for 10–12 min. After several rinses in TBS, the cells were permeabilized and blocked for 2 h in 0.2% (v/v) Triton X-100 (Sigma-Aldrich Corp.) and 10% (v/v) NDS (EMD Millipore) in TBS (pH 7.4) at RT. The neurons were incubated with primary antibody (rabbit anti-KCC2, 1:300; EMD Millipore) diluted in 10% (v/v) NDS at 4 °C overnight. After several rinses in TBS, the neurons were incubated with the corresponding secondary antibodies (donkey anti-rabbit conjugated to Alexa Fluor 488, 1:300; Molecular Probes) diluted in 10% (v/v) NDS at RT. The neurons were then rinsed several times in TBS for ≥ 30 min and mounted on slides with coverslips using ProLong Gold antifade reagent (Molecular Probes). The slides were viewed under an Olympus FV1000 confocal microscope with 60 × oil immersion objective, and the images were analyzed with Olympus Fluoview v.1.6a (Olympus Corp.).

Western blotting

Rat brain slices were dissociated, and the hippocampus was isolated on ice under a dissecting microscope and quickly homogenized in precooled lysis buffer (#K268–50; BioVision, Milpitas, CA, USA). The plasma membrane protein fractions were prepared from the homogenate using a standard procedure supplied with the membrane protein extraction kit purchased from BioVision (#K268–50). The membrane fractions were dissolved in 0.5% (v/v) Triton X-100 in PBS and inactivated by immersion in sodium dodecyl sulfate (SDS) sample buffer at 45 °C for 45 min. Membrane proteins were separated by SDS-polyacrylamide gel electrophoresis, electrophoretically transferred to polyvinylidene fluoride membranes (EMD Millipore), incubated with primary antibodies (anti-KCC2, 1:20,000, EMD Millipore; and β-actin, 1:1000, Cell Signaling Technology, Danvers, MA, USA) in 5% (v/v) skim milk-TBS-T (20 mM Tris (pH 7.6), 137 mM NaCl, and 0.05% (v/v) Tween 20) overnight at 4 °C, and finally incubated with peroxidase-conjugated Affinipure goat anti-rabbit (1:20,000; Jackson Laboratory, Bar Harbor, ME, USA) or rabbit anti-goat (1:20,000; Jackson Laboratory) secondary antibody in TBS-T buffer. After washing thrice in TBS-T, the bands were visualized with an enhanced chemiluminescence detection system (Thermo Fisher Scientific). Immunoreactivity of the individual bands was measured with Image-Pro Plus and normalized to β-actin.

Statistical analysis

All results are reported as mean ± SEM and statistical analysis was performed by SPSS 19.0. One sample test was used to compare the experimental group data which is presented as percent of control with 100%. A Chi Square test (χ^2 test) was used to compare the portion of bursting neurons in vitro and morality rate in vivo. One-way ANOVA

was used to compare across multiple experimental groups and multiple comparisons were corrected using Bonferroni post hoc test. Corresponding nonparametric analysis (Kruskal-Wallis one way ANOVA) was used to compare across multiple experimental groups if data were not normally distributed and multiple comparisons were corrected using Bonferroni post hoc test.

Results

FUR prevented CTZ-induced mKCC2 downregulation in both in vivo and in vitro acute seizure models

We verified whether FUR pretreatment had any effect on CTZ-induced mKCC2 reduction. In our previous studies, we dicoverd that intracerebroventricular CTZ injection could dose dependently and effectively induce typical seizure behaviors (Kong et al., 2010), and, also evoked significant downregulation of hippocampal mKCC2, but only in animals with ≥Racine score III seizure behavior (Chen et al., 2017). In this respect, in our current study, hippocampal tissues were isolated from those rats displaying at least Racine level 3 seizure behaviors 24 h after CTZ injection, similar as described in our previous study (Chen et al., 2017), and then, WB experiment was performed to determine the change of hippocampal CA1 area membrane KCC2 expression level in different pre-treatment animal groups. Our results showed there was a significant reduction in membrane level of KCC2 protein expression in CTZ group (CTZ: 57.6 ± 1.1%, n = 4, $P < 0.001$, one sample test, Fig. 1A) to its vehicle control level, similar as previous reported (Chen et al., 2017). In contrast, FUR alone did not induce any observable seizure behaviors either in FUR treatment group or in its pretreatment group within 30 min period, and FUR itself also had no effect on mKCC2 expression relative to the control (FUR: 97.5 ± 3.5%, n = 3, Fig. 1A). Interestingly, CTZ injection followed by the FUR pretreatment no longer evoked any mKCC2 reduction with the mKCC2 at a level similar to that of the DMSO control (FUR+CTZ: 104.0 ± 3.7%, n = 4, Fig. 1A), although FUR+CTZ group animals displayed similar seizure behavior level (all with Racine 3 or above seizure) as those in the CTZ alone group ($P > 0.05$). This result showed that FUR pretreatment significantly reversed CTZ-induced mKCC2 reduction ($P < 0.05$, Kruskal–Wallis one-way ANOVA, Fig. 1A).

FUR co-treatment (100 μM, 2 h) also significantly reversed 50 μM CTZ-induced mKCC2 downregulation in brain slices preparation. mKCC2 reduction by CTZ stimulation (CTZ: 58.9 ± 4.2% normalized to DMSO control, $P < 0.001$, one sample test, Fig. 1B) was significantly blocked by FUR co-incubation (FUR+CTZ: 97.0 ± 4.2%, $P < 0.001$, Kruskal–Wallis one-way ANOVA; Fig. 1B). Thus, both the in vivo and in vitro WB assays indicated that FUR pretreatment, while not affect the CTZ induced seizure, could block mKCC2 downregulation during convulsant CTZ stimulation.

FUR blocked CTZ-induced KCC2 immunosignal downregulation in hippocampal slices

Similar as in above stated in vivo seizure behavior experiemental precedures, another set of brain tissue, besides of WB experiment, was prepared for immunohistochemistry study, and the KCC2 immunofluorescence staining distribution in hippocampal slices is shown in Fig. 2A. For the control, a strong KCC2 immunoreactivity was observed in the CA1 area. KCC2 immunolabeling density after CTZ treatment was significantly reduced in both the soma and dendrite areas of the CA1 pyramidal cell layer. We also measured area-specific KCC2 immunofluorescence signal intensity. We compared each region in the CTZ, FUR, or FUR + CTZ groups with those in the DMSO group. The mean KCC2 labeling densities were decreased to 56.4 ± 2.7% in the pyramidal cell body layer ($P < 0.01$, one sample test; Figs. 2B), 48.7 ± 3.3% in the stratum radiatum ($P < 0.01$, one sample test; Fig. 2C), and 47.1 ± 6.5% in the stratum oriens ($P < 0.05$, one sample test; Fig. 2D) after CTZ treatment. FUR co-treatment significantly reversed CTZ-induced KCC2 reduction to 91.9 ± 5.9% in the pyramidal cell body layer ($P < 0.05$, one-way ANOVA) and 79.1 ± 7.0% in the stratum radiatum ($P < 0.05$, one-way ANOVA). FUR alone had no effect on KCC2 intensity either in the pyramidal cell body layer (91.4 ± 9.6%) or the stratum (oriens: 91.0 ± 4.8%; radiatum: 96.2 ± 4.0%) compared to that in the DMSO and FUR + CTZ groups. This in vitro immunostaining result further confirmed that FUR pretreatment protected CTZ induced seizure evoked KCC2 downregulation in the hippocampal CA1 area.

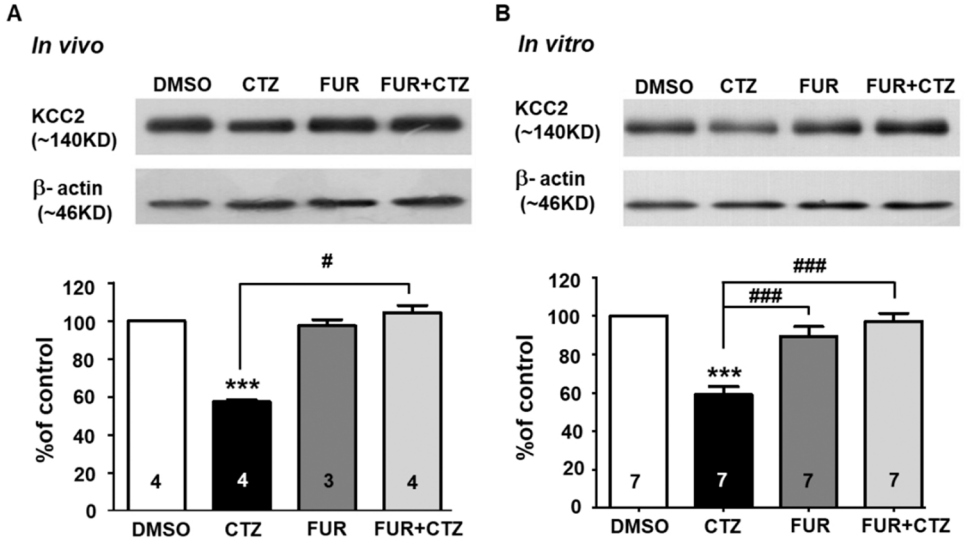

Fig. 1. FUR prevented mKCC2 downregulation in both in vivo and in vitro brain slice CTZ-induced acute seizure models. A: WB data showing significant hippocampal CA1 cell plasma KCC2 downregulation in rats presenting with seizures induced by CTZ treatment (i.c.v.) and FUR preinjection (i.c.v.) 15 min before CTZ prevented this. Tissue samples were collected at 24 h post CTZ injection of DMSO, CTZ, FUR, or FUR before CTZ. Top panel: representative WB bands cropped from same WB gel at ~140 kDa and ~46 kDa. Bottom panel: histogram showing quantification of mKCC2 expression in each group normalized to DMSO group. ($^{***}P < 0.001$ relative to DMSO, one sample test); Analysis by Kruskal-Wallis one way ANOVA revealed a significant difference of KCC2 expression among CTZ, FUR and FUR+CTZ groups ($P = 0.021$ across three groups, $^{\#}P < 0.05$, Kruskal-Wallis one way ANOVA with Bonferroni test). B: Representative WB bands showing quantity of mKCC2 in CA1 from hippocampal slices treated with either DMSO (0.1% v/v), CTZ (50 μM), FUR (100 μM) or CTZ + FUR, respectively, for 2 h. Bar plot showing quantification of KCC2 expression in each group normalized to DMSO-treated slices ($^{***}P < 0.001$ relative to DMSO, one sample test); Analysis by one-way ANOVA revealed a significant difference of KCC2 expression across CTZ, FUR and FUR+CTZ groups ($P < 0.001$ across three groups, $^{\#\#\#}P < 0.001$, one-way ANOVA with Bonferroni test).

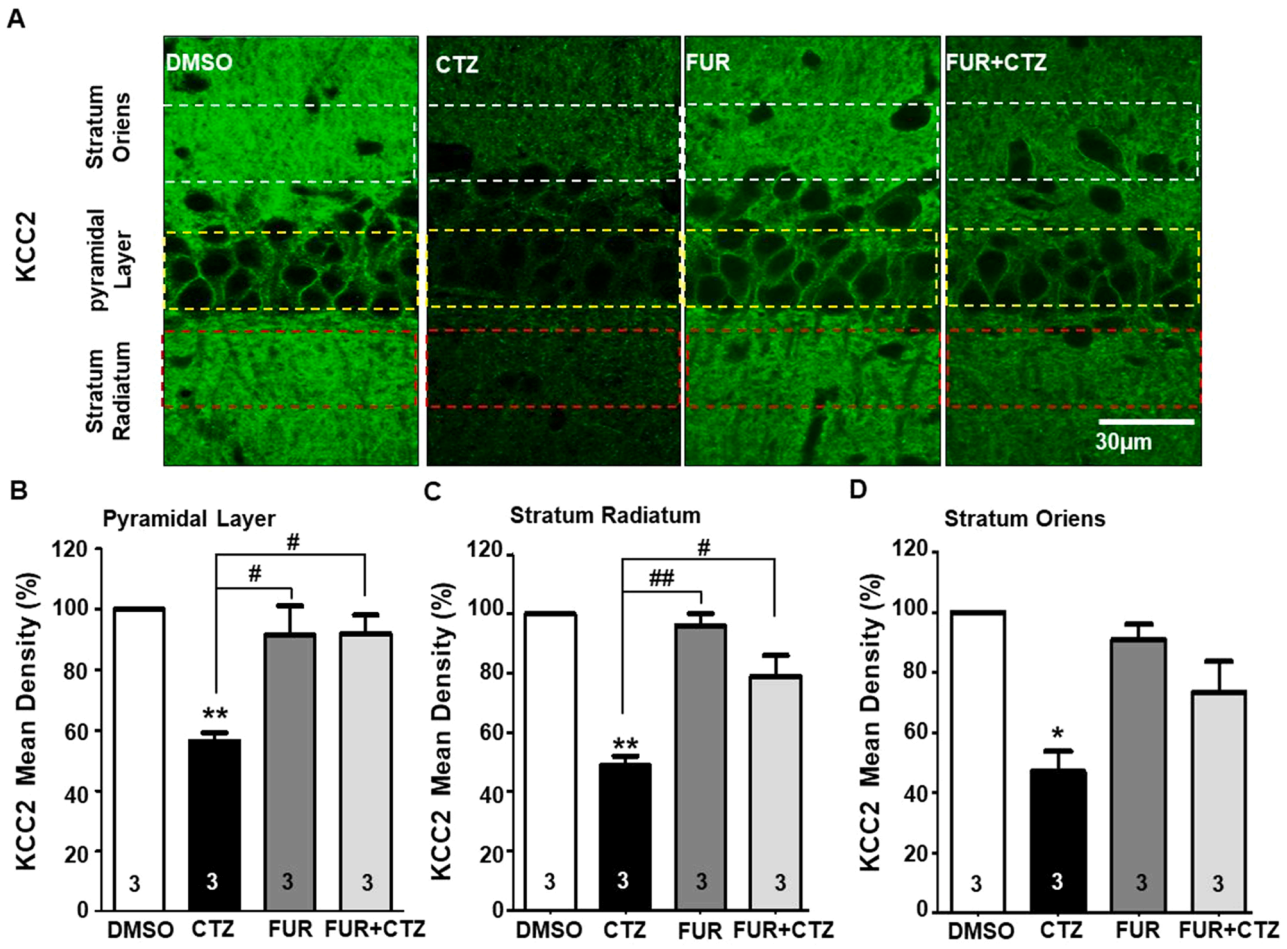

Fig. 2. FUR blocked CTZ-induced KCC2 immunosignal downregulation in hippocampal slices in vitro. A: Confocal microscope images showing hippocampal CA1 labeled with KCC2-specific antibody in DMSO, CTZ, FUR, or FUR + CTZ treatment group. Pronounced reduction in staining intensity was noted for CTZ treatment. Reduction was blocked by co-treatment with FUR. Scale bar, 30 μm. B–D: Bar plots showing quantification of KCC2 labeling density from marked areas in pyramidal layer (B) ($^{**}P < 0.01$ relative to DMSO, one sample test; $P = 0.016$ across CTZ, FUR, and FUR + CTZ groups, $^{\#}P < 0.05$, one-way ANOVA with Bonferroni test), Stratum radiatum (C) ($^{**}P < 0.01$ relative to DMSO, one sample test; $P = 0.002$ across CTZ, FUR, and FUR + CTZ groups, $^{\#}P < 0.05$, $^{\#\#}P < 0.01$, one-way ANOVA with Bonferroni test), and Oriens (D) (*P < 0.05 relative to DMSO, one sample test; $P = 0.078$, no significant differences among CTZ, FUR, and FUR + CTZ groups, Kruskal-Wallis one way ANOVA).

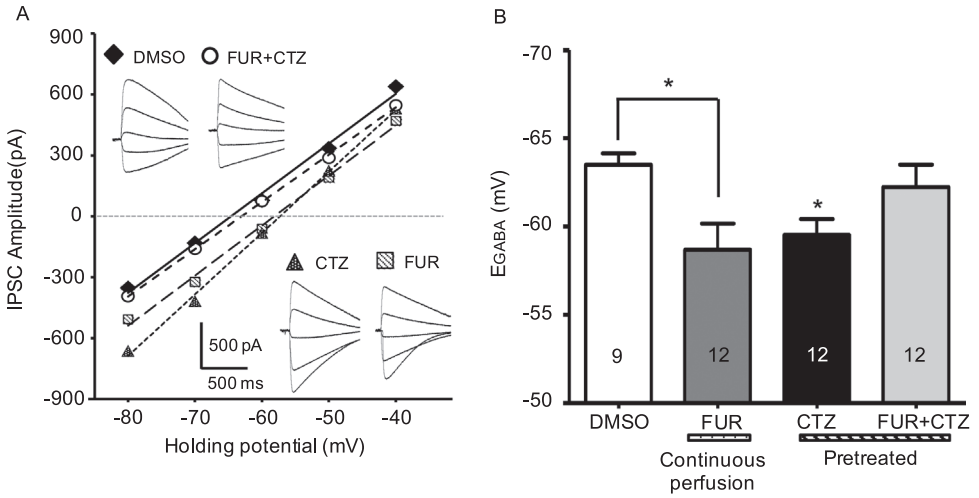

Fig. 3. FUR pretreatment prevented CTZ-induced positive E_{GABA} shift in CA1 pyramidal neurons. A: Representative patch clamp traces and plots showing postsynaptic currents evoked by puff GABA application at increasing holding potentials (starting at −80 mV in 10-mV increments) and peak GABAergic currents against holding potentials in pretreated DMSO, CTZ, CTZ + FUR groups and continuous perfusion FUR group. B: Histogram showing significant E_{GABA} depolarization shift with continuous FUR perfusion in comparison with DMSO ($^{*}P < 0.05$, *t*-test). A significant E_{GABA} depolarization shift was also observed in CTZ pretreatment group but not in CTZ + FUR pretreatment group ($P = 0.032$ across DMOS, CTZ, FUR+CTZ pretreatment groups; $^{*}P < 0.05$ one-way ANOVA with Bonferroni test).

FUR co-pretreatment reversed CTZ-induced EGABA positive shifts in CA1 pyramidal neurons

Under physiological conditions, KCC2 maintains Cl^- homeostasis, so that $GABA_AR$ can function normally as an inhibitor. Hence, E_{GABA} is a physiological indicator of mKCC2 function. Here, we measured E_{GABA} to investigate functional changes in mKCC2. Since WB and immunostaining above revealed that FUR blocked KCC2 downregulation induced by CTZ, we further tested whether FUR could also reverse the mKCC2 downregulation-induced E_{GABA} shift. As FUR itself is a KCC2 inhibitor (Hartmann et al., 2010; Loscher et al., 2013), we tested E_{GABA} shifts in bath solutions after FUR + CTZ co-treatment.

After 2 h of incubation, slices from the CTZ alone or FUR + CTZ groups were transferred into a recording chamber and perfused with normal ACSF during recording. For the FUR group, the tissues were continuously perfused with FUR during recording. IPSCs were evoked by puff application of GABA at a step increasing the holding potential. E_{GABA} was disclosed by plotting an offline current-voltage curve (Fig. 3A). As expected, FUR alone continuous perfusion caused a significant depolarizing shift of E_{GABA} in the CA1 pyramidal neurons relative to the control (DMSO: -63.5 ± 0.6 mV, n = 9 vs. FUR: -58.7 ± 1.5 mV; n = 12; $P < 0.05$, *t*-test; Fig. 3B). After rinsing off the CTZ alone or FUR + CTZ treatment, a significant depolarizing E_{GABA} shift continued to be recorded in the CTZ alone pretreatment groups (DMSO: -63.5 ± 0.6 mV, n = 9 vs. CTZ: -59.5 ± 0.9 mV, n = 12; $P < 0.05$, one-way ANOVA) but not in the FUR co-pretreatment groups (FUR + CTZ: -62.2 ± 1.3 mV, n = 12; $P > 0.05$, one-way ANOVA, Fig. 3B). The positive E_{GABA} shift induced by CTZ alone pretreatment indicated prolonged mKCC2 downregulation. However, it was attenuated by FUR co-pretreatment.

FUR co-pretreatment attenuated CTZ-induced decreases in the GABAergic current in CA1 pyramidal neurons

We further investigated whether CTZ-induced reduction in GABAergic inhibition is affected by FUR co-pretreatment. We recorded the mIPSC of the hippocampal CA1 pyramidal neurons in bath solutions for 2 h after drug treatment (Fig. 4A). Across three groups, there were significant differences in mIPSC amplitude ($P < 0.001$, Kruskal–Wallis one-way ANOVA) and mIPSC frequency ($P = 0.008$, Kruskal–Wallis one-way ANOVA), and then multiple comparisons were used to further reveal the differences between the groups. The amplitude was significantly lower in the neurons with the CTZ alone pretreatment (DMSO: 39.3 ± 1.8 pA, n = 20 vs. CTZ: 24.5 ± 1.6 pA, n = 13, $P < 0.001$; Fig. 4B). However, the decrease in mIPSC amplitude induced by CTZ was significantly reversed in the neurons with FUR co-pretreatment (FUR + CTZ: 33.3 ± 2.1 pA, n = 12 vs. CTZ: 24.5 ± 1.6 pA, n = 13, $P < 0.05$). A decrease in mIPSC frequency was also observed in the neurons with the CTZ alone pretreatment (DMSO: 2.4 ± 0.3 Hz vs. CTZ: 1.3 ± 0.3 Hz, $P = 0.01$; Fig. 4C). Nevertheless, FUR co-pretreatment did not block CTZ-induced mIPSC frequency reduction (FUR + CTZ: 1.7 ± 0.4 Hz, vs. CTZ: 1.3 ± 0.3 Hz, $P = 1.0$). This result indicates that the FUR-mediated protection of mKCC2 downregulation could rescue convulsant stimulation-induced KCC2 deficit-related $GABA_AR$ function impairment in the seizure induction phase.

Suppression of CTZ-induced epileptiform activity in cultured neurons by FUR

Our previous research demonstrated that inhibition of endogenous KCC2 expression promotes spontaneous epileptiform burst activity, whereas KCC2 overexpression inhibits it (Chen et al., 2017). Since the results above indicated that FUR could prevent mKCC2 downregulation induced by convulsant stimulation, we hypothesized that mKCC2 stabilized by FUR could enhance the inhibitory function of $GABA_AR$ and block the persistent epileptiform burst activity triggered by the convulsant.

To test this hypothesis, we performed electrophysiological recordings on cultured hippocampal neurons. DMSO (0.1%) as control, CTZ (5 μM) alone, or FUR (100 μM) + CTZ (5 μM) was applied to DIV 11

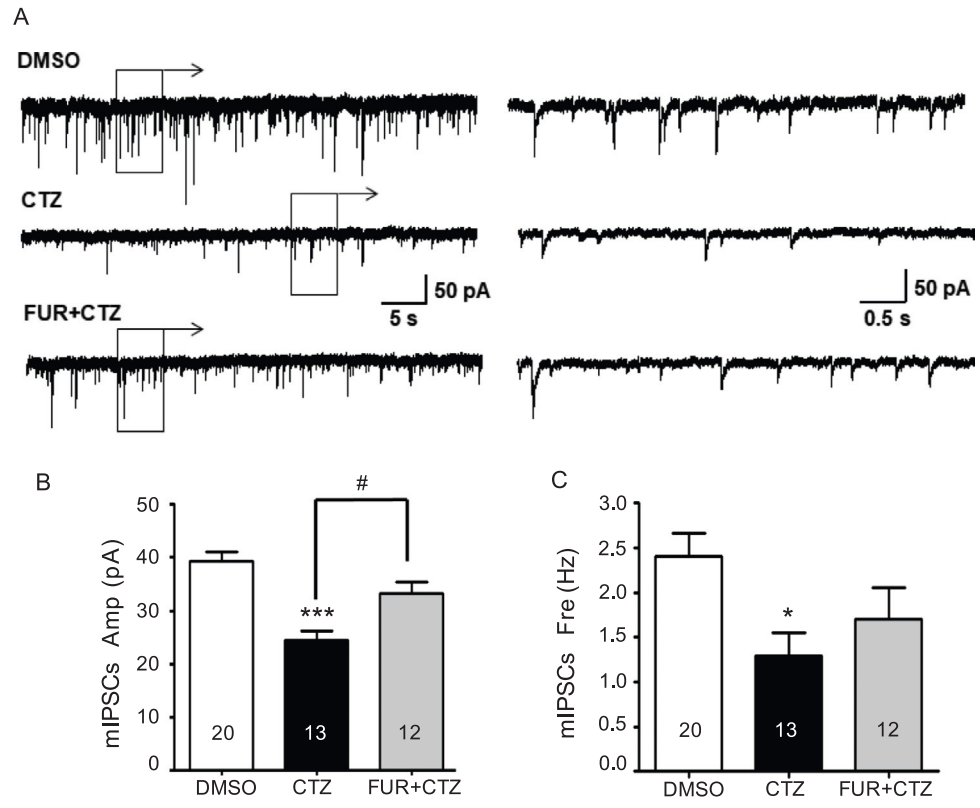

Fig. 4. FUR pretreatment attenuated CTZ-induced GABAergic mIPSC decrease in CA1 pyramidal neurons. A: Representative mIPSCs traces for CA1 pyramidal neurons after hippocampal slices pretreated with either DMSO (0.1% v/v), CTZ (50 μM), or FUR (100 μM) + CTZ (50 μM) for 2 h. B: Group data showing that significant decrease in mIPSC amplitude was induced in CTZ-pretreated neurons but prevented by FUR + CTZ co-pretreatment for 2 h followed by washout ($P<0.001$ across three groups, $^{***}P<0.001$ relative to DMSO; $\#P<0.05$ relative to CTZ, Kruskal-Wallis one-way ANOVA with Bonferroni test). C: Group data showing apparent reduction in mIPSC frequency was also observed in CTZ-pretreated neurons but could not be blocked by FUR pretreatment ($P=0.008$ across three groups, $^{*}P<0.05$ relative to DMSO, Kruskal-Wallis one-way ANOVA with Bonferroni test).

cultured hippocampal neurons for 48 h as drug pretreatments. We then performed immunocytochemistry on some of these neuron cultures and fixed them for KCC2 immunostaining. The KCC2 labeling in the DMSO control neurons displayed a typical uniform band pattern along the cell surface as previously reported (Chen et al., 2017). However, there was considerably less staining in neurons after the CTZ treatment (Fig. 5A). Quantitation analysis showed that mKCC2 expression was significantly reduced after CTZ treatment (DMSO: 100%, n = 5 batches vs. CTZ: 60.2 ± 3.2%, n = 5 batches; $P < 0.001$, one-sample test; Fig. 5B). However, KCC2 downregulation was significantly reversed by FUR co-treatment (FUR + CTZ: 82.5 ± 7.0%, n = 5 batches vs. CTZ: 60.2 ± 3.2%, n = 5 batches; $P<0.05$, *t*-test; Fig. 5B). These immunostaining results validated our previous in vivo and in vitro experimental observations and indicated that cultured neurons may also be suitable for the study of mKCC2 downregulation during convulsant stimulation.

We transferred the coverslips with cultured neurons to a drug-free bath solution for whole-cell patch recording and used current clamp recording to evaluate neuronal epileptiform activity under various drug treatments. Epileptiform burst activity consists of > 5 consecutive action potentials overlaying a depolarizing shift of ≥ 10 mV that lasts ≥ 300 ms. A neuron with at least two repeated burst activities that occurred during the 10 min recording period is considered to be an epileptiform bursting neuron, as defined in previous studies (Chen et al., 2017; Qi et al., 2006; Wang et al., 2009). Analysis by Chi-square showed that the portion of bursting neurons among three groups are significantly different ($P = 0.0011$). Similar to our earlier study (Chen et al., 2017), CTZ alone pretreatment here induced epileptiform bursting activity in the cultured neurons (Fig. 5C) and significantly elevated the proportion of bursting neurons in comparison to DMSO pretreatment (CTZ: 12/13, 92.3% vs. DMSO: 5/19, 26.3%; $P < 0.05$, χ^2 test with Bonferroni test, Fig. 5D). In the FUR + CTZ pretreatment group, however, the proportion of bursting neurons was a slight increase but no significant difference in comparison to that in the DMSO group (14/25, 56%; $P > 0.05$ relative to DMSO, χ^2 test with Bonferroni test, Fig. 5D), and a reduction trend in comparison to that in the CTZ alone group ($P > 0.05$ relative to CTZ, χ^2 test with Bonferroni test, Fig. 5D).

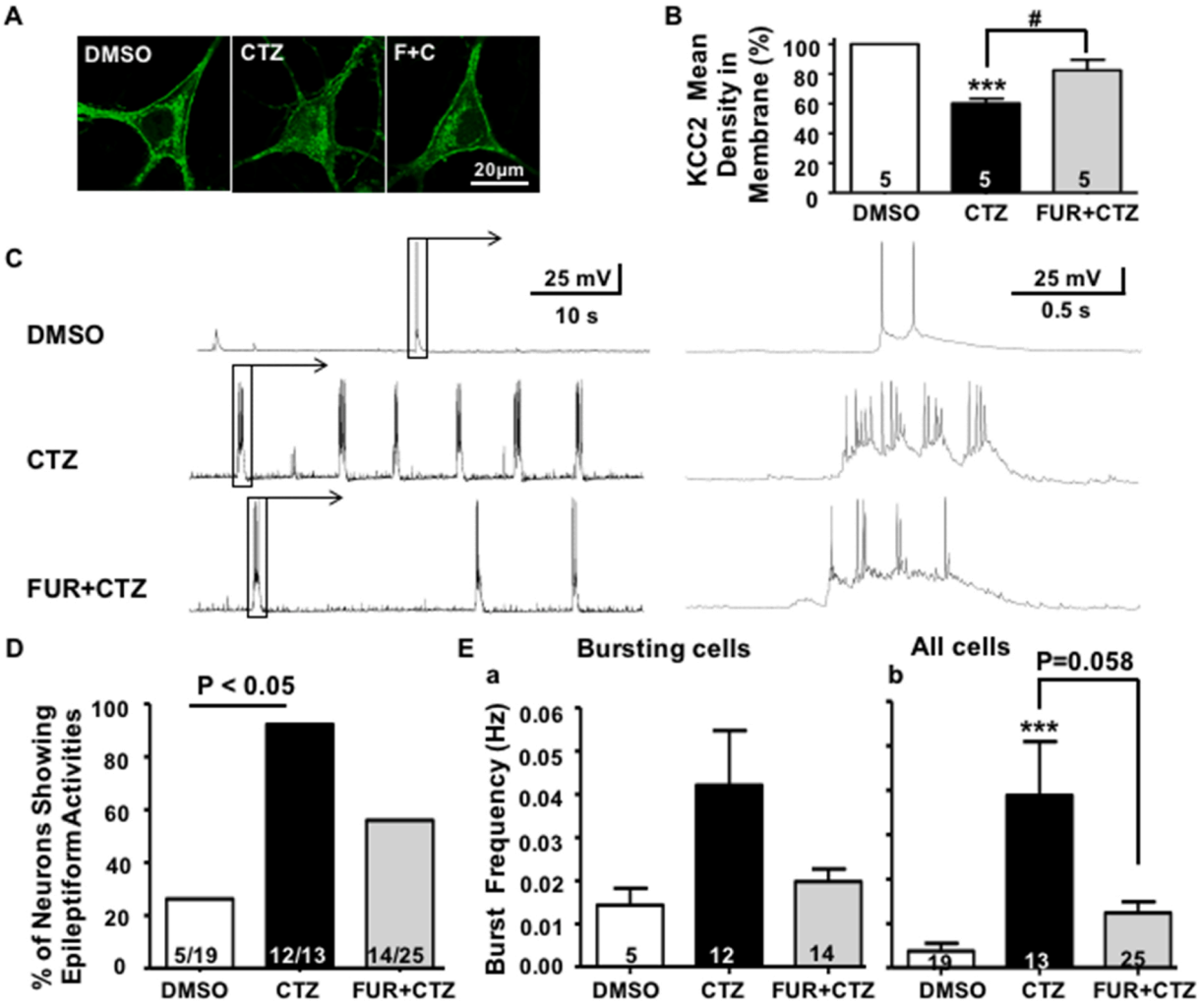

Fig. 5. Suppression of CTZ-induced epileptiform activity in cultured hippocampal neurons by FUR pretreatment. A: Confocal microscope images showing cultured hippocampal neurons labeled with KCC2 after treatment with DMSO (0.1% v/v), CTZ (5 μM), FUR (100 μM), or CTZ + FUR, respectively. B: Quantification of KCC2 labeling density (number of labeled pixel surfaces per somatic perimeter) ($^{***}P < 0.01$ relative to DMSO, one sample test; $^{\#}P < 0.05$ relative to CTZ, *t*-test). C: Representative current clamp traces recorded from neurons pretreated with DMSO, CTZ, or FUR + CTZ for 48 h and normal bath solution during recording. D: Group data showing that washout of CTZ after 48 hr treatment still significantly increased the portion of bursting neurons, while washout of FUR+CTZ after 48 hr treatment reduced % of bursting neurons and had no significant difference in comparison with DMSO ($P = 0.0011$ across three groups; DMSO vs. CTZ, $P < 0.05$, χ^2 test with Bonferroni test). E: (a) Group data analysis showed no significant differences of burst frequency in bursting cells from three groups (Kruskal-Wallis one-way ANOVA); (b) Group data analysis showed significant increase of burst frequency in all recording cells from CTZ group ($P = 0.001$ across three groups, $^{***}P < 0.001$ relative to DMSO, Kruskal-Wallis one-way ANOVA with Bonferroni test). FUR decreased burst frequency after washout ($P = 0.058$, Kruskal-Wallis one-way ANOVA with Bonferroni test).

We analyzed the influence of CTZ alone and FUR + CTZ co-pretreatment on neuronal burst frequency (Hz). In all the assessed neurons (Fig. 5E(B)), the burst frequency in the CTZ group (0.039 ± 0.012 Hz, n = 13) was significantly higher than that in the DMSO group (0.004 ± 0.002 Hz, n = 19, $P < 0.001$, Kruskal–Wallis one-way ANOVA). However, the burst frequency in the FUR + CTZ groups was only 0.011 ± 0.003 (n = 25) and not significantly different from that in the DMSO group ($P = 0.164$, Kruskal–Wallis one-way ANOVA). It was, however, somewhat lower than that in the CTZ group ($P = 0.058$, Kruskal–Wallis one-way ANOVA), indicating that FUR pretreatment had the tendency to decrease neuronal mKCC2 and suppress epileptiform burst activity. This result further confirmed that FUR stabilized mKCC2, enabled its rapid functional recovery, and suppressed abnormal epileptiform burst activity.

Effects of FUR pretreatment on CTZ-induced acute seizure animal model

To test whether FUR pretreatment influences CTZ convulsant stimulation in vivo, we performed in vivo experiments on rats with CTZ injections (i.c.v.) with or without FUR pre-injection (i.c.v.). Consistent with previous studies (Chen et al., 2017; Kong et al., 2010), seizure behaviors at different maximum seizure levels were observed in most animals during the acute CTZ induction period. Racine score III or above epileptic seizures were observed in 96% (23/24) of the rats (Figs. 6a, 6b). Similarly, in the FUR + CTZ group, up to 90% of rats (17/19) showed epileptic seizure behavior as expected, since acute FUR application would only inhibit KCC2 function before it was cleared from the local brain region. The mean maximal Racine scores were similar for both groups (CTZ: 4.5 ± 0.2, n = 24 vs. FUR + CTZ: 3.9 ± 0.3, n = 19, $P = 0.12$; Fig. 6C). Among those rats showing Racine score III or above seizure behaviors, we examined whether FUR altered seizure latency after CTZ injection. The latencies in the FUR + CTZ and the CTZ alone groups were 21.5 ± 10.3 min (n = 17) and 22.2 ± 10.7 min (n = 23), respectively ($P = 0.38$; Fig. 6D). Therefore, inhibition of KCC2 function by FUR had no added effect on the CTZ-induced acute seizures. This result further proved that there was no difference in the severity of seizures in either the CTZ alone or FUR+ CTZ group, which provides a basis for further study. However, within 24 h after CTZ injection, the mortality rate in the FUR + CTZ group was significantly lower than that in the CTZ alone group (CTZ: 46%, n = 24 vs. FUR + CTZ: 16%, n = 19, * $P < 0.05$, χ^2 test; Fig. 6E). In fact, detailed analysis showed that within the first 1.5 h of the acute induction period, there was no remarkable difference in mortality between the CTZ alone (5/24, 21%) and the FUR + CTZ groups (3/19, 16%; Fig. 6E). However, while acute seizures were terminated with chloral hydrate 1.5 h after CTZ injection, no animals died between 1.5 h and 24 h in the FUR + CTZ group, but six animals died in the CTZ alone group (CTZ: 6/19, 32% vs. FUR + CTZ: 0/16, 0%; * $P < 0.05$, χ^2 test; Fig. 6E). This result suggests that FUR, by stabilizing KCC2 on the cell membrane during acute convulsant stimulation, may have a protective effect on animals against convulsant stimulation-induced death.

Discussion

To further extend our previous reported observation, this current study elucidated a way, by using FUR, a KCC2 inhibitor, to effectively protect KCC2 downregulation in the neuronal membrane during seizures. Our results showed that FUR pretreatment counteracted

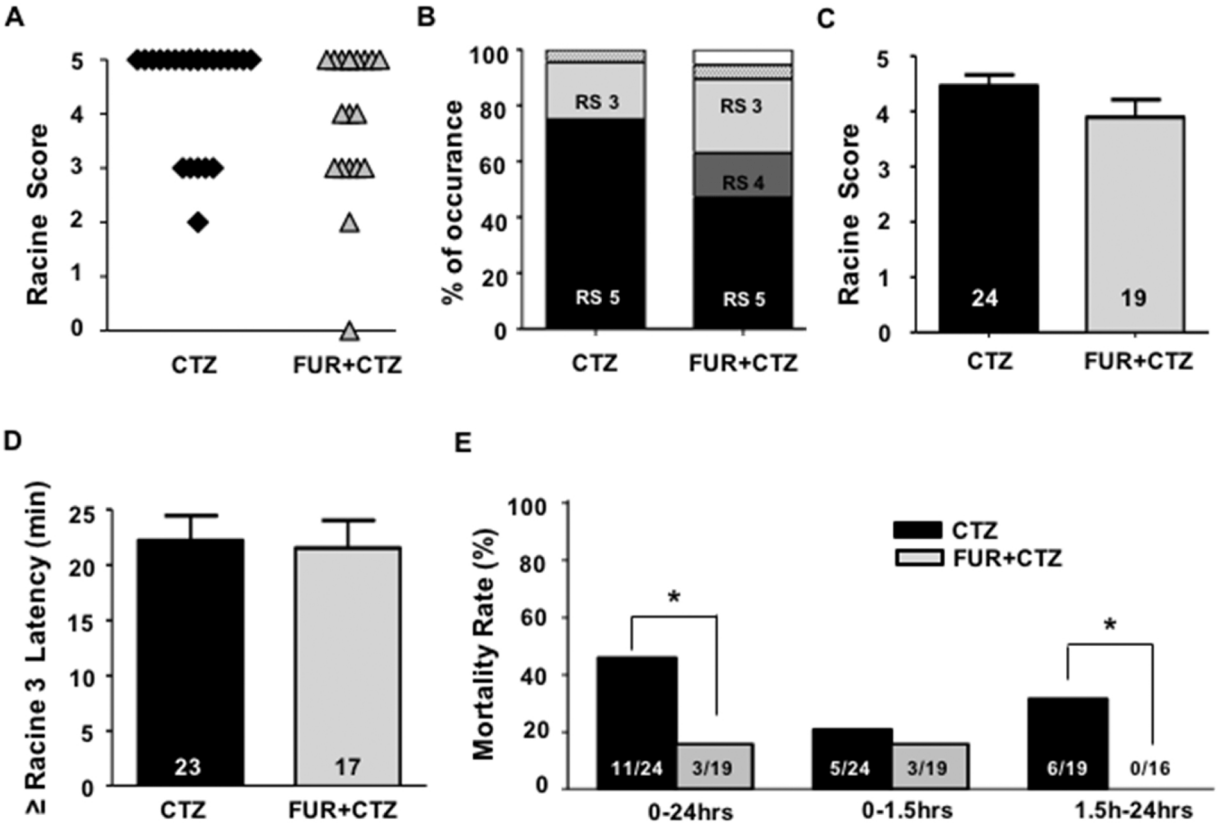

Fig. 6. Effects of FUR treatment on CTZ-induced acute seizure behavior and mortality rate in freely moving rats. A: Scatter plots showing seizure behavior scores for animals in CTZ and FUR + CTZ groups. B: Bar plots showing the percentage of rats with maximal Racine score behavior. C: Histograms showing mean maximal behavioral seizure scores of animals in CTZ and FUR + CTZ groups. D: Histograms showing latency of ≥ Racine-III seizure behavior. FUR did not decrease latency of CTZ-induced seizures. E: Histograms showing mortality rates of rats during and immediately after seizure induction by CTZ injection (*$P < 0.05$ relative to CTZ, ***t***-test).

convulsant stimulation-induced mKCC2 reduction and stabilized the membrane during seizures both in vivo and in vitro. Since KCC2 is important in the regulation of $GABA_AR$, normal mKCC2 expression could help recover impaired GABA inhibition during convulsant stimulation and counteract seizures.

Surface KCC2 expression and normal Cl^- extrusion ensure normal GABA inhibitory function. mKCC2 downregulation and KCC2 dysfunction perturb Cl^- homeostasis, causing a depolarization shift in E_{GABA}, reduce GABA inhibition, and facilitate epileptogenesis (Huberfeld et al., 2007). FUR has been extensively administered as a non-selective pharmacological KCC2 inhibitor. It has been used to assess and mimic E_{GABA} shifts (Barmashenko et al., 2011; Pathak et al., 2007). FUR application in the range of 0.1–1 mM to control granule neurons mimicked the E_{GABA} positive shift in pilocarpine-induced status epilepticus neurons (Pathak et al., 2007). GABA-activated hyperpolarization currents in DIV 14–21 hippocampal neurons were abolished by 100 μM FUR but rapidly reversed by washing it out (Lee et al., 2011). Previous studies have focused on functional inhibition mediated by FUR, however, no prior research has explored whether FUR affects KCC2 expression. Here in our current study, similar as previous reported (Wan et al., 2020), 100 μM FUR showed the depolarization shift of the E_{GABA} which suggested an inhibition on KCC2 in mature neurons. But the effect of 100 μM FUR is suspected to result from inhibition of both KCC2 and NKCC1, since FUR also serves as an inhibitor for NKCC1, and the inhibition constant (Ki) for KCC2 and NKCC1 is 25 μM (Payne, 1997) and 40 μM (Gillen et al., 1996), respectively. Although in mature neurons, the expression of NKCC1 is extremely low, we still need to consider to exclude the influence of NKCC1 effect in our current study. Selective blockage of NKCC1 using low concentrations of bumetanide strongly affects neuronal Cl^- in both immature and mature hippocampal CA3 neurons (Tyzio et al., 2008), modifies Cl^- dependent GABAergic neurotransmission and decreases severity of epileptic activity (Ben-Ari, 2017; Kahle et al., 2008; Loscher et al., 2013). While in our previous study, the effect of FUR on surface NKCC1 is negligible owing to low basal expression level in mature neurons and rare upregulation in hippocampal slices during CTZ-induced epileptiform activity (Chen et al., 2017). Both CTZ (50 μM/2 hr) and FUR (100 μM /2 hr) treatment resulted in a depolarization shift of E_{GABA}, but not by bumetanide (10 μM /2 hr) (Chen et al., 2017). Moreover, our unpublished data found that FUR could facilitate the formation of evoked potentials and shorten the latency of double peaks in CA1 area of hippocampus induced by CTZ, but bumetanide blocking NKCC1 activity specifically did not affect the process of evoked potential. Besides, VU0463271, a recently developed selective inhibitor of KCC2, has been used and demonstrated that inhibition of KCC2 alone could cause depolarizing shift in E_{GABA} values and increase of epileptiform activity (Sivakumaran et al., 2015). Thus, we performed similar experiments by using CTZ + VU0463271, and the results showed that VU0463271 co-treatment did indeed also protect membrane KCC2 downregulation, and suppress bursting activities similar as FUR co-treatment with CTZ after washing out in CTZ in vitro model (supplementary Fig. S1). FUR rapidly and reversibly inhibits KCC2 by binding to its large extracellular loop (LEL) (Hartmann et al., 2010; Loscher et al., 2013). However, the precise LEL binding site for FUR is unknown. The conserved cysteine residues C287, C302, C322, and C331 in LEL play important roles in KCC2 function. Substitution of any of these residues abolished KCC2 transport activity but did not alter KCC2 expression (Come et al., 2019; Hartmann and Nothwang, 2014; Hartmann et al., 2010). Therefore, FUR might suppress KCC2 function while maintaining mKCC2 expression by binding and blocking one or more of the aforementioned cysteine residues.

mKCC2 trafficking steps including delivery, diffusion, clustering, endocytosis, recycling, and/or degradation are regulated by the phosphorylation of key residues (Chamma et al., 2013; Heubl et al., 2017; Kahle et al., 2013; Kaila et al., 2014; Lee et al., 2011, 2007, 2010b; Puskarjov et al., 2012; Watanabe et al., 2009; Zhou et al., 2012). Tyrosine 903/1087 (Y903/1087), serine 940 (S940), and threonine 906/1007 (T906/1007) are distributed in the carboxy terminal domain required to stabilize the membrane (Come et al., 2019; Friedel et al., 2017). S940 phosphorylation is required for stability and normal function (Silayeva et al., 2015). Inhibition of S940 phosphorylation suppresses KCC2 and increases the latency and severity of status seizures induced by KA in vivo (Silayeva et al., 2015). In contrast, KCC2 is upregulated by reducing (T906/T1007) phosphorylation which, in turn, limits epileptiform activity (Moore et al., 2018). Under physiological conditions, mKCC2 turnover is ~20–30 min, while its lifetime is thought to be more than 4 h because of several turnover cycles before its final degradation (Come et al., 2019; Lee et al., 2010b; Puskarjov et al., 2012). Under pathological conditions, activity-dependent KCC2 endocytosis and degradation rapidly decrease mKCC2 (Chamma et al., 2013; Come et al., 2019; Heubl et al., 2017; Lee et al., 2011). Our previous study showed that S940 phosphorylation and mKCC2 significantly declined 2 h after CTZ application to hippocampal slices (Chen et al., 2017). In a 0 Mg^{2+} model, the inhibition of S940 dephosphorylation by a PP1 inhibitor prevented mKCC2 internalization. Nevertheless, downregulation was significantly reversed by blocking m-calpain over activation (Wan et al., 2018). The present study results seemed to indicate that FUR counteracted internalization and degradation mediated by S940 dephosphorylation and m-calpain over activation. FUR stabilized KCC2 may avoid the long-term endocytosis-degradation pathway and could be recovered to normal function upon FUR clearance.

Earlier in vivo studies have shown that intravenous or intraperitoneal FUR injections had antiepileptic efficacy (Ahmad et al., 1976; Haglund and Hochman, 2005; Hesdorffer et al., 2001; Reid et al., 2000; Yamada et al., 2013). FUR may also synergistically enhance the efficacy of other antiepileptic drugs (Luszczki et al., 2007). FUR is rapidly metabolized and the blood–brain barrier (BBB) is relatively impermeable to it (Pacifici, 2012; Roesner, 1986; Yang et al., 2009). Hence, its putative antiepileptic mode of action is increasing the ECS, limiting neuronal swelling, and inhibiting the transmission of epileptiform electrical activity through gap junctions under pathological conditions (Haglund and Hochman, 2005; Hochman et al., 1995, 1999). Intravenous mannitol administration increased ECS osmolality and inhibited spontaneous and stimulation-evoked epileptic activity in the neocortex (Haglund and Hochman, 2005). We then examined whether neuronal KCC2 is implicated in FUR antiepileptic efficacy. Here, we used FUR injection (i.c.v.) to avoid net FUR diffusion by the BBB. The other problem for this study is the compound used, CTZ and FUR, of which both have solubility issue. FUR and CTZ in physiological solution is very low, and we performed solution preparation very carefully, and as recommended in solvent DMSO first. In our experiments, FUR and CTZ powder was firstly dissolved in DMSO to make 200 mM and 100 mM stock solution. Then an equal volume of ASCF was slowly added and then ultrasounded to enhance dissolving process to form 100 mM FUR and 50 mM CTZ working solution, and clear solution, by visual observation, without any precipitation was finally obtained. In addition, we did perform simple observation to look under microscope instead of visual observation, of the final solution of CTZ + FUR, and as we expected, no particles could be seen in this test solution. In in vitro experiments, working solution of either FUR or CTZ was sequentially slowly added into the large amount ASCF to make the final incubation solution with continuously stirring, and any precipitation was carefully monitored to ensure both drugs were fully dissolved into the ACSF. During in vivo experiment of i.c.v injection, 100 mM FUR working solution was injected first and then, 15 min later CTZ was then injected. By using this combined drug injection protocol, the seizure score and the latency in FUR + CTZ group was no difference to CTZ alone group, indicating that CTZ could maintain the effective concentration to generate acute seizure induction in FUR + CTZ group. Strikingly, it was found that FUR maintained survivability after acute seizure termination with chloral hydrate. The in vitro assay confirmed that after CTZ and FUR co-pretreatment and removal, the proportions of hippocampal neurons presenting with epileptiform and burst frequency activity were

significantly decreased. Furthermore, VU0463271 co-treatment did indeed protect membrane KCC2 downregulation and suppressed bursting activities similar a FUR co-treatment with CTZ in CTZ in vitro model (supplementary Fig. S1). In summary, all these procedures and controls strongly suggest that the effect of FUR blockade of KCC2 downregulation during CTZ seizure induction is unlikely of FUR directly intervene with CTZ molecule to induce neuronal epileptiform activity, rather than FUR somehow prevented CTZ induced neuronal excitation evoked membrane KCC2 downregulation.

The in vivo behavioral study here disclosed no significant effect of FUR on seizure induction during the acute phase. However, the mortality rates were significantly higher in non-FUR pretreated CTZ model rats during the recovery period (1.5–24 h) after cessation of seizure behavior. This phenomenon, first, is unlikely owing to FUR interference with the CTZ-induced acute seizure, since in the acute induction phase, neither the seizure score nor the seizure latency had differences between these two groups. Further, from the widely accepted view of the functional property of FUR as a KCC2 inhibitor, it would inhibit the KCC2 function to reduce $GABA_AR$ function, hence, enhancing convulsant-induced seizure probabilities (Chen et al., 2017). Thus, to explain this epilepsy-suppressing phenomenon, we hypothesized that mKCC2 protected by the FUR could, after FUR was washed away, functionally enhance the inhibitory function of the remaining GABA receptors in the epileptic brain area to protect against epileptiform brain excitation-induced death. Although the minor antiepileptic effect of FUR was only observed in the acute seizure model in our current study, it is worthwhile to explore whether FUR may have protective effects by reducing recurrent seizures in a chronic seizure model. However, in the current study, we did not generate data on seizure occurrence during the chronic period, owing to the model that we used (CTZ model) (Kong et al., 2014; Kong et al., 2010) and the time limits in our current study. Thus, a study to investigate whether protection of mKCC2 from downregulation during early induction phase of the acute seizure may interrupt the epileptogenesis process is needed in future.

The major shortfall of this study is that it did not investigate the mechanism underlying the protective effect of FUR on mKCC2. KCC2 is a glycoprotein with 12 transmembrane segments, including a long intracellular C-terminal domain vital to membrane stability, a short intracellular amino terminal domain essential for KCC2 membrane delivery, and six extracellular loops (Come et al., 2019; Friedel et al., 2017). KCC2 is downregulated in seizure patients and animal models (Cohen et al., 2002; Huberfeld et al., 2008, 2007; Lee et al., 2010a; Palma et al., 2006; Pathak et al., 2007; Rivera et al., 2002), probably because of its S940A phosphorylation. Maintenance of KCC2 expression or function during epileptic activities could be an effective way to interrupt or even terminate epileptogenesis (Silayeva et al., 2015). However, the effect of FUR on keeping KCC2 on the cell membrane during convulsant stimulation seems antithetical to the inhibitory nature of KCC2. However, our explanation, although we do not have experimental evidence, is that to function as a KCC2 inhibitor, FUR has to bind to one or several extracellular loops of KCC2, and this may in turn change the three-dimensional structure of KCC2 and hence interrupting the effect of S940 dephosphorylation during convulsant stimulation. Indeed, previous studies have already shown that besides its KCC2 inhibitor properties, FUR exerted anticonvulsant effects both in vitro (Gutschmidt et al., 1999; Hochman and Schwartzkroin, 2000; Margineanu and Klitgaard, 2006) and in vivo (Ahmad et al., 1976; Haglund and Hochman, 2005; Hesdorffer et al., 2001; Hochman et al., 1995; Reid et al., 2000; Yamada et al., 2013). Thus, we hypothesize that this anticonvulsant function of FUR might be attributable to its protection of KCC2 downregulation during convulsant stimulation and subsequent enhancement of $GABA_AR$ function. Nevertheless, the exact mechanism of FUR inhibition of KCC2 downregulation during convulsant stimulation needs to be further studied.

Conclusion

During epileptogenesis, the dynamic KCC2 plasticity change, an early stage downregulation and late stage recovery in epileptic neurons, has been attributed to as one of the major contributors to the chronic seizure. Preventing KCC2 downregulation in the early stage may interrupting the process of epileptogenesis after initial epileptiform stimulation in nature. In the current study, we discovered that FUR could stabilize mKCC2 and prevent the usual downregulation of KCC2 during convulsant stimulation in hippocampal neurons. The stabilization of mKCC2 may rapidly recover KCC2 function, enhance GABA receptor efficiency after seizure stimulation, and impede progression from acute seizure to epileptogenesis. Our results provide a new avenue for interrupting epileptogenesis by blocking mKCC2 downregulation.

Funding

This work was funded by Nature Science Foundation of China (NSFC) grants (32111530119, 81971204, 31771188 and 81873787), and supported by Shanghai Municipal Science and Technology Major Project (No. 2018SHZDZX01), ZJ Lab, and Shanghai Center for Brain Science and Brain-Inspired Technology. It also supported by a grant from Natural Science Foundation of Shanghai [No. 18ZR1424800] to XZ, and a grant from Shenzhen Science and Technology Innovation Commission Municipality (JCYJ20210324103409023) to LW.

CRediT authorship contribution statement

LC, LW, XL, XZ and YW conceived the study design. LC, BQ, JZ, ZH, JY, and XL established the animal model, prepared the brain slices, performed the patch clamp recordings, and conducted the immunostaining. BQ, JZ, LW performed western blotting. LC, ZW and XL conducted the patch clamp recordings. GW performed the cell culture. LC, LW, JY, and ZW analyzed the data. LC, LW, XL, JZ, XZ, and YW wrote, commented and modified the manuscript. All authors approved the final version of the manuscript.

Declarations of interest

None.

Appendix A. Supporting information

Supplementary data associated with this article can be found in the online version at doi:10.1016/j.ibneur.2022.04.010.

References

Ahmad, S., Clarke, L., Hewett, A.J., Richens, A., 1976. Controlled trial of frusemide as an antiepileptic drug in focal epilepsy. Br. J. Clin. Pharmacol. 3, 621–625.
Barbaro, N.M., Takahashi, D.K., Baraban, S.C., 2004. A potential role for astrocytes in mediating the antiepileptic actions of furosemide in vitro. Neuroscience *128*, 655–663.
Barmashenko, G., Hefft, S., Aertsen, A., Kirschstein, T., Kohling, R., 2011. Positive shifts of the GABA(A) receptor reversal potential due to altered chloride homeostasis is widespread after status epilepticus. Epilepsia *52*, 1570–1578.
Ben-Ari, Y., 2002. Excitatory actions of GABA during development: the nature of the nurture. Nature Rev. Neurosci. 3, 728–739.
Ben-Ari, Y., 2017. NKCC1 chloride importer antagonists attenuate many neurological and psychiatric disorders. Trends Neurosci. 40, 536–554.
Chamma, I., Heubl, M., Chevy, Q., Renner, M., Moutkine, I., Eugene, E., Poncer, J.C., Levi, S., 2013. Activity-dependent regulation of the K/Cl transporter KCC2 membrane diffusion, clustering, and function in hippocampal neurons. J. Neurosci. 33, 15488–15503.
Chen, L., Wan, L., Wu, Z., Ren, W., Huang, Y., Qian, B., Wang, Y., 2017. KCC2 downregulation facilitates epileptic seizures. Scientific Rep. 7, 156.
Cohen, I., Navarro, V., Clemenceau, S., Baulac, M., Miles, R., 2002. On the origin of interictal activity in human temporal lobe epilepsy in vitro. Science *298*, 1418–1421.
Come, E., Heubl, M., Schwartz, E.J., Poncer, J.C., Levi, S., 2019. Reciprocal regulation of KCC2 trafficking and synaptic activity. Front. Cell Neurosci. 13, 48.

Farrant, M., Nusser, Z., 2005. Variations on an inhibitory theme: phasic and tonic activation of GABA(A) receptors. Nat. Rev. Neurosci. 6, 215–229.
Friedel, P., Ludwig, A., Pellegrino, C., Agez, M., Jawhari, A., Rivera, C., Medina, I., 2017. A novel view on the role of intracellular tails in surface delivery of the potassium-chloride cotransporter KCC2. eNeuro 4.
Gillen, C.M., Brill, S., Payne, J.A., Forbush 3rd, B., 1996. Molecular cloning and functional expression of the K-Cl cotransporter from rabbit, rat, and human. A new member of the cation-chloride cotransporter family. J. Biol. Chem. 271, 16237–16244.
Gutschmidt, K.U., Stenkamp, K., Buchheim, K., Heinemann, U., Meierkord, H., 1999. Anticonvulsant actions of furosemide in vitro. Neuroscience *91*, 1471–1481.
Haglund, M.M., Hochman, D.W., 2005. Furosemide and mannitol suppression of epileptic activity in the human brain. J. Neurophysiol. 94, 907–918.
Hartmann, A.M., Nothwang, H.G., 2014. Molecular and evolutionary insights into the structural organization of cation chloride cotransporters. Front. Cell Neurosci. 8, 470.
Hartmann, A.M., Wenz, M., Mercado, A., Storger, C., Mount, D.B., Friauf, E., Nothwang, H.G., 2010. Differences in the large extracellular loop between the K(+)-Cl(-) cotransporters KCC2 and KCC4. J. Biol. Chem. 285, 23994–24002.
Hesdorffer, D.C., Stables, J.P., Hauser, W.A., Annegers, J.F., Cascino, G., 2001. Are certain diuretics also anticonvulsants? Ann. Neurol. 50, 458–462.
Heubl, M., Zhang, J., Pressey, J.C., Al Awabdh, S., Renner, M., Gomez-Castro, F., Moutkine, I., Eugene, E., Russeau, M., Kahle, K.T., et al., 2017. GABAA receptor dependent synaptic inhibition rapidly tunes KCC2 activity via the Cl(-)-sensitive WNK1 kinase. Nat. Commun. 8, 1776.
Hochman, D.W., Baraban, S.C., Owens, J.W., Schwartzkroin, P.A., 1995. Dissociation of synchronization and excitability in furosemide blockade of epileptiform activity. Science *270*, 99–102.
Hochman, D.W., D'Ambrosio, R., Janigro, D., Schwartzkroin, P.A., 1999. Extracellular chloride and the maintenance of spontaneous epileptiform activity in rat hippocampal slices. J. Neurophysiol. 81, 49–59.
Hochman, D.W., Schwartzkroin, P.A., 2000. Chloride-cotransport blockade desynchronizes neuronal discharge in the "epileptic" hippocampal slice. J. Neurophysiol. 83, 406–417.
Huberfeld, G., Clemenceau, S., Cohen, I., Pallud, J., Wittner, L., Navarro, V., Baulac, M., Miles, R., 2008. Epileptiform activities generated in vitro by human temporal lobe tissue. Neurochirurgie 54, 148–158.
Huberfeld, G., Wittner, L., Clemenceau, S., Baulac, M., Kaila, K., Miles, R., Rivera, C., 2007. Perturbed chloride homeostasis and GABAergic signaling in human temporal lobe epilepsy. J. Neurosci. 27, 9866–9873.
Inoue, M., Uriu, T., Otani, H., Hara, M., Omori, K., Inagaki, C., 1989. Intracerebroventricular injection of ethacrynic acid induces status epilepticus. Eur. J. Pharmacol. 166, 101–106.
Jacob, T.C., Moss, S.J., Jurd, R., 2008. GABA(A) receptor trafficking and its role in the dynamic modulation of neuronal inhibition. Nat. Rev. Neurosci. 9, 331–343.
Jefferys, J.G., 1990. Basic mechanisms of focal epilepsies. Exp. Physiol. 75, 127–162.
Kahle, K.T., Deeb, T.Z., Puskarjov, M., Silayeva, L., Liang, B., Kaila, K., Moss, S.J., 2013. Modulation of neuronal activity by phosphorylation of the K-Cl cotransporter KCC2. Trends Neurosci. 36, 726–737.
Kahle, K.T., Staley, K.J., Nahed, B.V., Gamba, G., Hebert, S.C., Lifton, R.P., Mount, D.B., 2008. Roles of the cation-chloride cotransporters in neurological disease. Nat. Clin. Pract. Neurol. 4, 490–503.
Kaila, K., Price, T.J., Payne, J.A., Puskarjov, M., Voipio, J., 2014. Cation-chloride cotransporters in neuronal development, plasticity and disease. Nat. Rev. Neurosci. 15, 637–654.
Kong, S., Cheng, Z., Liu, J., Wang, Y., 2014. Downregulated GABA and BDNF-TrkB pathway in chronic cyclothiazide seizure model. Neural Plast *2014*, 310146.
Kong, S., Qian, B., Liu, J., Fan, M., Chen, G., Wang, Y., 2010. Cyclothiazide induces seizure behavior in freely moving rats. Brain Res. 1355, 207–213.
Lee, H.H., Deeb, T.Z., Walker, J.A., Davies, P.A., Moss, S.J., 2011. NMDA receptor activity downregulates KCC2 resulting in depolarizing GABAA receptor-mediated currents. Nat. Neurosci. 14, 736–743.
Lee, H.H., Jurd, R., Moss, S.J., 2010a. Tyrosine phosphorylation regulates the membrane trafficking of the potassium chloride co-transporter KCC2. Mol. Cell Neurosci. 45, 173–179.
Lee, H.H., Walker, J.A., Williams, J.R., Goodier, R.J., Payne, J.A., Moss, S.J., 2007. Direct protein kinase C-dependent phosphorylation regulates the cell surface stability and activity of the potassium chloride cotransporter KCC2. J. Biol. Chem. 282, 29777–29784.
Lee, H.H.C., Jurd, R., Moss, S.J., 2010b. Tyrosine phosphorylation regulates the membrane trafficking of the potassium chloride co-transporter KCC2. Mol. Cell Neurosci. 45, 173–179.
Liu, X., Chen, B., Chen, L., Ren, W.T., Liu, J., Wang, G., Fan, W., Wang, X., Wang, Y., 2013. U-shape suppressive effect of phenol red on the epileptiform burst activity via activation of estrogen receptors in primary hippocampal culture. PLoS One *8*, e60189.
Loscher, W., Puskarjov, M., Kaila, K., 2013. Cation-chloride cotransporters NKCC1 and KCC2 as potential targets for novel antiepileptic and antiepileptogenic treatments. Neuropharmacology *69*, 62–74.
Luszczki, J.J., Sawicka, K.M., Kozinska, J., Borowicz, K.K., Czuczwar, S.J., 2007. Furosemide potentiates the anticonvulsant action of valproate in the mouse maximal electroshock seizure model. Epilepsy Res. 76, 66–72.
Margineanu, D.G., Klitgaard, H., 2006. Differential effects of cation-chloride co-transport-blocking diuretics in a rat hippocampal slice model of epilepsy. Epilepsy Res. 69, 93–99.
McCormick, D.A., Contreras, D., 2001. On the cellular and network bases of epileptic seizures. Annu. Rev. Physiol. 63, 815–846.
Moore, Y.E., Deeb, T.Z., Chadchankar, H., Brandon, N.J., Moss, S.J., 2018. Potentiating KCC2 activity is sufficient to limit the onset and severity of seizures. Proc Natl Acad Sci U. S. A. 115, 10166–10171.
Nakahata, Y., Miyamoto, A., Watanabe, M., Moorhouse, A.J., Nabekura, J., Ishibashi, H., 2010. Depolarizing shift in the GABA-induced current reversal potential by lidocaine hydrochloride. Brain Res. 1345, 19–27.
Pacifici, G.M., 2012. Clinical pharmacology of the loop diuretics furosemide and bumetanide in neonates and infants. Paediatr Drugs *14*, 233–246.
Palma, E., Amici, M., Sobrero, F., Spinelli, G., Di Angelantonio, S., Ragozzino, D., Mascia, A., Scoppetta, C., Esposito, V., Miledi, R., et al., 2006. Anomalous levels of Cl- transporters in the hippocampal subiculum from temporal lobe epilepsy patients make GABA excitatory. Proc. Nat. Acad. Sci. U. S. A. 103, 8465, 103, 11814-11814.
Pathak, H.R., Weissinger, F., Terunuma, M., Carlson, G.C., Hsu, F.C., Moss, S.J., Coulter, D.A., 2007. Disrupted dentate granule cell chloride regulation enhances synaptic excitability during development of temporal lobe epilepsy. J. Neurosci. 27, 14012–14022.
Payne, J.A., 1997. Functional characterization of the neuronal-specific K-Cl cotransporter: implications for [K+](0) regulation. Am. J. Physiol. Cell Physiol. 273, C1516–C1525.
Puskarjov, M., Ahmad, F., Kaila, K., Blaesse, P., 2012. Activity-dependent cleavage of the K-Cl cotransporter KCC2 mediated by calcium-activated protease calpain. J. Neurosci. 32, 11356–11364.
Qi, J., Wang, Y., Jiang, M., Warren, P., Chen, G., 2006. Cyclothiazide induces robust epileptiform activity in rat hippocampal neurons both in vitro and in vivo. J. Physiol. 571, 605–618.
Racine, R., Okujava, V., Chipashvili, S., 1972. Modification of seizure activity by electrical stimulation. 3. Mechanisms. Electroencephalogr. Clin. Neurophysiol. 32, 295–299.
Reid, K.H., Guo, S.Z., Iyer, V.G., 2000. Agents which block potassium-chloride cotransport prevent sound-triggered seizures in post-ischemic audiogenic seizure-prone rats. Brain Res. 864, 134–137.
Rivera, C., Li, H., Thomas-Crusells, J., Lahtinen, H., Viitanen, T., Nanobashvili, A., Kokaia, Z., Airaksinen, M.S., Voipio, J., Kaila, K., et al., 2002. BDNF-induced TrkB activation down-regulates the K+-Cl- cotransporter KCC2 and impairs neuronal Cl- extrusion. J. Cell. Biol. 159, 747–752.
Rivera, C., Voipio, J., Payne, J.A., Ruusuvuori, E., Lahtinen, H., Lamsa, K., Pirvola, U., Saarma, M., Kaila, K., 1999. The K+/Cl- co-transporter KCC2 renders GABA hyperpolarizing during neuronal maturation. Nature *397*, 251–255.
Rivera, C., Voipio, J., Thomas-Crusells, J., Li, H., Emri, Z., Sipila, S., Payne, J.A., Minichiello, L., Saarma, M., Kaila, K., 2004. Mechanism of activity-dependent downregulation of the neuron-specific K-Cl cotransporter KCC2. J. Neurosci. 24, 4683–4691.
Roesner, M., 1986. The loop diuretics: focus on furosemide and ethacrynic acid. N C Med. J. 47, 93–96.
Silayeva, L., Deeb, T.Z., Hines, R.M., Kelley, M.R., Munoz, M.B., Lee, H.H., Brandon, N.J., Dunlop, J., Maguire, J., Davies, P.A., et al., 2015. KCC2 activity is critical in limiting the onset and severity of status epilepticus. Proc. Natl. Acad. Sci. U. S. A. 112, 3523–3528.
Sivakumaran, S., Cardarelli, R.A., Maguire, J., Kelley, M.R., Silayeva, L., Morrow, D.H., Mukherjee, J., Moore, Y.E., Mather, R.J., Duggan, M.E., et al., 2015. Selective inhibition of KCC2 leads to hyperexcitability and epileptiform discharges in hippocampal slices and in vivo. J. Neurosci. 35, 8291–8296.
Tyzio, R., Minlebaev, M., Rheims, S., Ivanov, A., Jorquera, I., Holmes, G.L., Zilberter, Y., Ben-Ari, Y., Khazipov, R., 2008. Postnatal changes in somatic gamma-aminobutyric acid signalling in the rat hippocampus. Eur. J. Neurosci. 27, 2515–2528.
Wake, H., Watanabe, M., Moorhouse, A.J., Kanematsu, T., Horibe, S., Matsukawa, N., Asai, K., Ojika, K., Hirata, M., Nabekura, J., 2007. Early changes in KCC2 phosphorylation in response to neuronal stress result in functional downregulation. J. Neurosci. 27, 1642–1650.
Wan, L., Chen, L., Yu, J., Wang, G., Wu, Z., Qian, B., Liu, X., Wang, Y., 2020. Coordinated downregulation of KCC2 and GABAA receptor contributes to inhibitory dysfunction during seizure induction. Biochem. Biophys. Res. Commun. 532, 489–495.
Wan, L., Ren, L., Chen, L., Wang, G., Liu, X., Wang, B.H., Wang, Y., 2018. M-calpain activation facilitates seizure induced KCC2 down regulation. Front. Mol. Neurosci. 11, 287.
Wang, Y., Qi, J.S., Kong, S., Sun, Y., Fan, J., Jiang, M., Chen, G., 2009. BDNF-TrkB signaling pathway mediates the induction of epileptiform activity induced by a convulsant drug cyclothiazide. Neuropharmacology *57*, 49–59.
Watanabe, M., Wake, H., Moorhouse, A.J., Nabekura, J., 2009. Clustering of neuronal K+-Cl- cotransporters in lipid rafts by tyrosine phosphorylation. J. Biol. Chem. 284, 27980–27988.
Yamada, J., Zhu, G., Okada, M., Hirose, S., Yoshida, S., Shiba, Y., Migita, K., Mori, F., Sugawara, T., Chen, L., et al., 2013. A novel prophylactic effect of furosemide treatment on autosomal dominant nocturnal frontal lobe epilepsy (ADNFLE). Epilepsy Res. 107, 127–137.
Yang, K.H., Choi, Y.H., Lee, U., Lee, J.H., Lee, M.G., 2009. Effects of cytochrome P450 inducers and inhibitors on the pharmacokinetics of intravenous furosemide in rats: involvement of CYP2C11, 2E1, 3A1 and 3A2 in furosemide metabolism. J. Pharm. Pharmacol. 61, 47–54.
Zhou, H.Y., Chen, S.R., Byun, H.S., Chen, H., Li, L., Han, H.D., Lopez-Berestein, G., Sood, A.K., Pan, H.L., 2012. N-methyl-D-aspartate receptor- and calpain-mediated proteolytic cleavage of K+-Cl- cotransporter-2 impairs spinal chloride homeostasis in neuropathic pain. J. Biol. Chem. 287, 33853–33864.